Effect of heat treatment on microstructure, hardness and tensile properties of high-speed selective laser melted Ti6Al4V

Paul Lekoadi[1*], *Monnamme* Tlotleng[1,2], *Kofi* Annan[3], *Nthabiseng* Maledi[4] and *Bathusile* Masina[1,2]
[1]CSIR Photonics Centre, Manufacturing Cluster, P O Box 395, Pretoria 0001, South Africa
[2]University of Johannesburg, Mechanical Engineering Science Department, Johannesburg 2012, South Africa
[3]University of Pretoria, Material Science and Metallurgical Engineering Department, Pretoria, South Africa
[4]University of the Witwatersrand, School of Chemical and Metallurgical Engineering, Johannesburg, Private Bag X3, 2050, South Africa

Abstract. This study presents the investigation of the influence of heat treatment on microstructure, hardness and tensile properties of high-speed selective laser melted Ti6Al4V components. Heat treatment was performed to obtain an improved microstructure with enhanced hardness and tensile properties. It was found that the acicular martensitic α′ structure on the as-built sample lead to high hardness, yield strength and ultimate tensile strengths of 389±10 $HV_{0.3}$, 949 ± 10 MPa and 1045 ± 3 MPa, respectively, with a low ductility of 5%. Heat treatment transformed the martensitic α′ structure into lamella α + β phases, with heat treatment at 1000 °C resulting in the most improved hardness and ductility from 389 ± 10 $HV_{0.3}$ and 5% to 325 ± 20 $HV_{0.3}$ and 13%, and a decrease in yield and ultimate tensile strength from 949 ± 10 MPa and 1045 ± 13MPa to 835 ± 11 MPa and 911 ± 5 MPa, respectively.

1 Introduction

The Ti6Al4V components manufactured with selective laser melting (SLM) technique have shown great potential in various industries which include aerospace, aeronautics, automobile, military [1-3], due to their favourable properties such as outstanding strength-to-weight ratio, good corrosion resistance, high fracture toughness and biocompatibility [4, 5]. Ti6Al4V is a dual-phase alloy, with both the hexagonal close packed (hcp) α-phase and body centred cubic (bcc) β-phase coexisting at room temperature [6]. The manufacturing of Ti6Al4V with SLM technique offers a variety of important advantages which include high level of flexibility, near net shape production, manufacturing of complex geometries, time and material savings, which cannot be achieved by traditional conventional manufacturing techniques [7-9]. Detailed description of the fundamental processing of SLM are discussed elsewhere [10].

* PLekoadi@csir.co.za

SLM manufactured Ti6Al4V components undergo repeated melting and solidification (solidification rates in the range of 10^3 - 10^5K/s) when the powder is fused by high energy laser source [11, 12]. As a result, non-equilibrium phase transformation from β phase to an unstable martensite α′ phase is promoted, which results in the formation of a fully martensitic α' microstructure [13, 14]. Therefore, SLM manufactured Ti6Al4V parts in their as-built state possess fully martensitic α′ microstructure, which is characterised by high residual stresses, microstructural inhomogeneity and poor mechanical properties including mechanical anisotropy, high hardness, and low tensile ductility [12, 15, 16]. It is well known that post-processing heat treatment is often carried out to eliminate the residual stresses, improve the microstructure, mitigate mechanical anisotropy and improve tensile ductility, thereby transforming the unstable martensite α′ phase into stable α + β phases [17-19].

Heat treatment of SLM manufactured Ti6Al4V components can present various types of microstructures with different heat treatment parameters. It is understood that both lamella and bimodal α + β microstructures are favourable in Ti6Al4V for aerospace application, since lamella microstructure offers excellent fracture toughness and high resistance to fatigue crack propagation, whereas bimodal microstructure offers outstanding combination of strength and ductility [20-22]. This implies that, in order to obtain a fully transformed α + β microstructure via post-processing heat treatment, it is important to understand and select heat treatment parameters such as temperature, residence time and cooling medium for the improvement of the microstructure and mechanical properties of SLM Ti6Al4V [23]. In a previous study [23], the effect of heat treatment parameters (i.e., temperature, residence time and cooling method) on microstructure and hardness properties of SLM Ti6Al4V were evaluated.

A study by Bai et al. [12] evaluated the effect of heat treatment on microstructure and mechanical properties of SLM Ti6Al4V cuboid samples that were manufactured using laser power of 280 W, scanning speed of 1400 mm/s, hatch spacing of 110 μm and layer thickness of 30 μm. Various heat treatments using temperatures ranging from 850-1020 °C at various residence times in the range of 0.5-2 h followed by furnace cooling (FC) were studied. It was reported that both lamella and bimodal microstructures were achieved after heat treatment, whereby the bimodal microstructure gave a yield strength (YS) of 1054 ± 9.6 MPa and ductility of 9.8 ± 1.8%, with the results considered as a good combination of strength and ductility. Moreover, it was reported that annealing at 950 °C produced a lamella microstructure with the highest fracture toughness of 90.8 ± 2.1 $MPa^{1/2}$. It was further reported that tensile properties of Ti6Al4V is dependent on the size and morphology of α phase, which increased with annealing temperature.

A study by Jin et al. [1] also reported on the effect of heat treatment on microstructure and mechanical properties SLM manufactured Ti6Al4V. In the study, Ti6Al4V cubic samples were manufactured using laser power of 320 W, scanning speed of 1200 mm/s, spot size in the range 80-100 μm and layer thickness of 0.06 mm. The samples were heat treated to 750 °C, 850 °C, 920 °C and 1050 °C for 2.5 h and cooled by FC, while others were hot isostatically pressed (HIPed) to 920 °C at 120 MPa for 2,5 h followed by FC. It was found that the acicular martensite phase α′ gradually decomposes into α + β phases after annealing at temperatures higher that 850 °C. It was further reported that the YS decrease from 1119 MPa to 860 MPa, while the ultimate tensile strength (UTS) decreased from 1235 MPa to 1013 MPa as the annealing temperature increased in the range 750-1050 °C. However, the ductility increased from 8.3% to 15.7% after heat treatment at 920 °C, and slightly dropped to 15.4% after heat treatment at 1050 °C.

Zou et al. [24] investigated the influence of heat treatment on microstructure and tensile properties of SLM produced Ti6Al4V by conducting heat treatment on cylindrical Ti6Al4V samples that were produced using proprietary optimised process parameters. The samples were heat treated at temperatures in the range 925-1030 °C for a period of 2 h before they were cooled at a cooling rate of 7 °C/min. Their results showed that heat treatment at 925 °C

for 2 h led to a basket weave lamella α + β microstructure, found inside the columnar grains, with α-lamellae thickness of ~1.4 µm. The latter microstructure was characterized by YS of 833 ± 13 MPa, UTS of 913 ±13 MPa and ductility of 15.9 ± 0.8%, which was considered a good balance of strength and ductility. Finally, Li et al. [25] conducted multi-step heat treatment on cubic Ti6Al4V specimens that were manufactured with laser power of 90 W, scanning speed 450 mm/s, hatching space 80 µm and layer thickness 25 µm. The multi-step heat treatment was performed at temperatures in the range 650-950 °C for 2 h followed by FC. It was reported that heat treatment promoted transformation of the martensitic α′ structure into equiaxed α + β grain structure, with globular α-phase size of ~10 µm. According to the authors, the resulted equiaxed grain microstructure exhibited superior ductility of 21.8%, at the cost of YS and UTS to 900 MPa and 953 MPa, respectively.

The reviewed studies show that different heat treatment profiles lead to different microstructural characteristics which are obviously characterised by different mechanical properties. This implies that a broader considerate into the effect of other heat treatments on microstructure and mechanical properties is important and desired. Therefore, this study focused on investigating the effect of heat treatment on the microstructure and the resultant hardness and tensile properties of high speed SLM manufactured Ti6Al4V components.

2 Experimental procedure

2.1 Materials

Grade 5, pre-alloyed Ti6Al4V powder with particle size distribution (PSD) in the range 20-60 µm was used as a deposition material during printing of the samples. The powder was produced and supplied by TLS Technik GMbH & Co and was used as received. The Ti6Al4V powder show spherical morphology and smooth particles with PSD in the range 25-63 µm, with small satellite particles as can be seen in Figures 1(a) and (b), respectively. The samples were printed on a Ti6Al4V base plate.

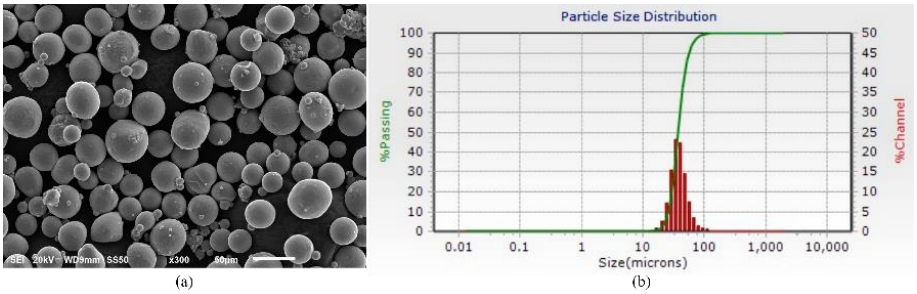

Fig. 1. (a) SEM image of the powder morphology of Ti6Al4V, (b) Particle size distribution of Ti6Al4V powder.

2.2 Methods

Cylindrical test samples with a length of 80 mm and diameter of 15mm were produced from Aeroswift 3D printing SLM machine that is available at the Council of Scientific and Industrial Research (CSIR) in Pretoria, South Africa. The Aeroswift machine was equipped with a high power 5 kW single Ytteribium laser, with a wavelength of 1076 nm and a build volume of 2000 mm x 600 mm x 600 mm. A bi-directional building strategy in the z-direction was used during printing of the samples. Before printing of the samples, the oxygen content

inside the building chamber was reduced to 300 ppm by purging with inert argon gas with purity of 99%. Furthermore, the base plate was pre-heated to a temperature of 200 °C. The Ti6Al4V powder was dried in an oven at 120 °C for 2 h in order to remove moisture before it was processed. Post sample manufacturing, the samples were removed from the base plate by cutting with wire cutter and prepared for heat treatment.

All samples were heat treated inside a STF 16/180 Carbolite horizontal tube furnace (manufactured by Parson Lane, England), with an internal tube diameter of 1 m. Before the heat treatment process commenced, the oxygen concentration inside the tube furnace was reduced to 100 ppm by continuously purging the chamber with argon gas to avoid contamination. The gas was continuously flowing at a constant gas flow rate of 2 L/min throughout the heat treatment process. To evaluate the effect of heat treatment, the samples were heat treated to temperatures of 950 °C and 1000 °C at a heating rate of 10 °C/min for 2 h and 8 h followed by furnace cooling (FC). A summary of the heat treatment profiles used is given in Table 1.

Table 1. Summary of heat treatment profiles.

Heat treatment no:	Temperature (°C)	Holding time (h)	Cooling method
HT-1	950	2	FC
HT-2	1000	2	FC
HT-3	1000	8	FC

After heat treatment, the samples were mounted on an AMP 50 automatic mounting press machine. An AKA Resin Phenolic SEM black conductive resin was used to mount all specimens. Mounted samples were mechanically grounded with Struers Tetrapol-25 grinding and polishing machine. Silicon carbide (SiC) grinding papers from grit size of 80, 320, 1200 and 4000 were used for grinding the specimens. Polishing of the specimens was conducted using Diapro MD-Mol 3µm diamond suspension for 3 min and colloidal silica 0.04 µm OP-S suspension for a period of 3 min as the final polishing stage. Cleaning of the polished specimens was prepared with soap suspension and dried with ethanol. The specimens were etched with Kroll's reagent, which is a solution containing 100 mL H_2O, 1-3 mL HF and 2-6 mL HNO_3. The etching time for all specimens was between 10-15 s.

The specimens were observed for microstructure using Joel JSM-6010PLUS/LA scanning electron microscope (SEM). Microstructural images were taken at 150X and 1500X magnifications. Microhardness measurements were conducted on Matsuzawa Seiko Vickers MTH-1 microhardness model machine. A force and dwell time of 300 gf and 10 seconds were used during measurements, respectively. For all samples, three hardness patterns were taken along the built direction (z-axis), and the average was calculated as the hardness of the material. All tensile measurements were performed on an Instron 1342 tensile testing machine. A constant crosshead of 0.5 mm/min was used throughout the measurements. All tensile specimens were machined to a standard cylindrical bar dog-bone shape. Tensile testing was conducted according to ASTM standard E8-E8M.

During testing, strain measurement was done by attaching the extensometer to the gauge section on the test specimen and the extensometer was removed at a strain of 5% to prevent damage during specimen fracture. Three tensile samples for each heat treatment profile were tested. Tensile test measurements were conducted at room temperature.

3 Results and discussions

3.1 Microstructure

The microstructures of the as-built and heat treated samples obtained under different conditions are presented in Figure 2. In order to investigate detailed information and for clear microstructural observation, zoomed in areas are indicated by a black square on the microstructures of the samples.

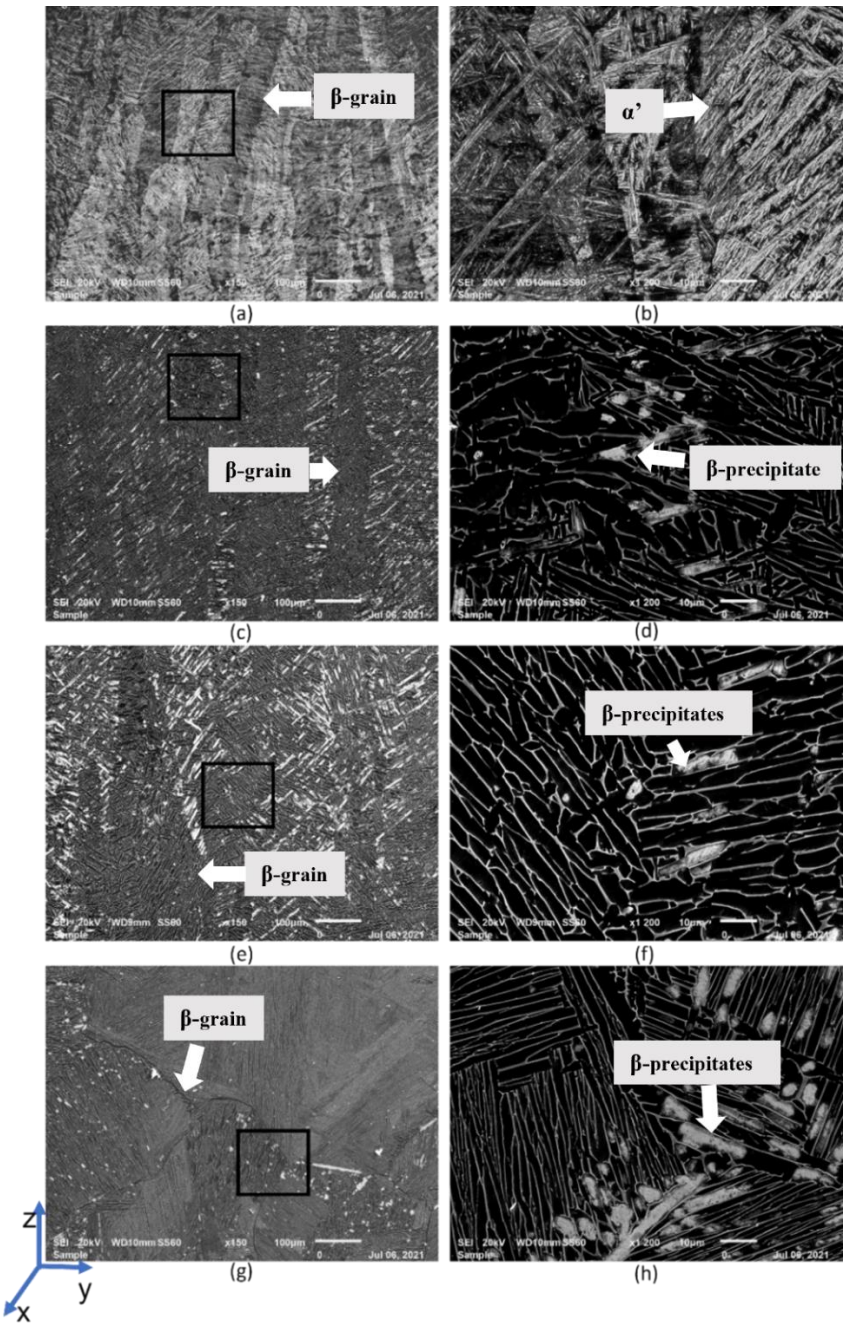

Fig. 2. SEM microstructures of the samples, (a, b) As-built, (c, d) HT-1, (e, f) HT-2, and (g, h) HT-3.

The microstructure of the as-built sample was characterised by long columnar β grains that were elongated along the built direction (z-direction) as can be seen in Figure 2(a). The columnar morphology of the β grains resulted from epitaxial growth that took place through nucleation on the top surface of previously deposited layers, through re-melting and re-solidification during SLM processing. A study by Liu et al. [6] reported that growth of the columnar β grain follows an overall downward heat flow direction, whose preferential

direction is <100> which is preferred by bcc lattice structure. Hence, prior β grains grow over many layers of building and reach several microns in height and width as can be seen in Figure 2(a). A sharp acicular α′ structure was observed inside these prior β grains and were randomly embedded as laths as shown in Figure 2(b). Since Ti6Al4V is a dual-phase α + β alloy, the formation of martensite α′ phase followed a diffusionless transformation from β-phase into α′ (β → α′) due to high cooling rates (~10^4-10^5 K/s) experienced by the sample during SLM processing [1, 6, 11, 24]. According to Bai et al. [12], the cooling rate of SLM process is much higher than the critical transformation rate of martensite α′ phase, which explains the existence of martensite α′ phase on the microstructure of SLM manufactured Ti6Al4V samples. Similar observation of forming a fully martensitic α′ microstructures were reported in literature on SLM manufactured Ti6Al4V components [23, 26, 27].

Phase transformation of the meta-stable martensitic α′ phase to stable lamella α + β phases (α′ → α + β) was observed after heat treatment at 950 °C as can be seen in Figure 2(c). It is important to note that even though phase transformation was evident, the columnar prior β grains remained visible (Figure 2c), which was an indication that the transformation was not completed [1]. However, the columnar prior β grains appear to a certain degree of damage as can be seen in Figure 2(c). According to the Ti6Al4V phase diagram presented in Figure 3, 950 °C is described as a temperature higher in the α + β region, but slightly below β-transus temperature [28], which explains the incomplete transformation.

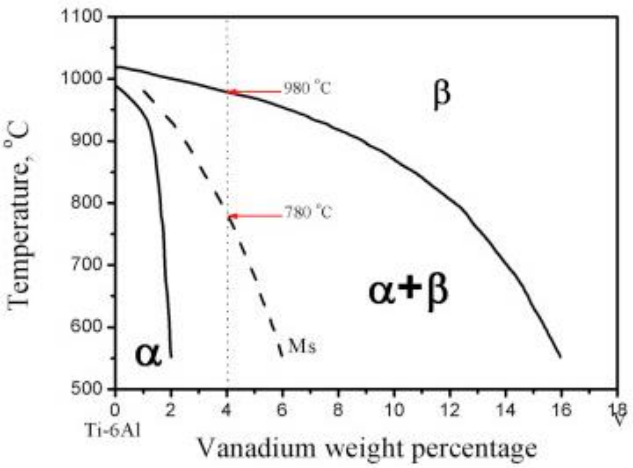

Fig. 3. The Ti6Al4V phase diagram [28].

Heat treatment at 950 °C also resulted in growth of the α and β phases at the boundaries of the prior β grains (Figure 2c). Moreover, heat treatment at 950 °C led to the formation of retained β precipitates as shown in Figure 2(d). Similar β precipitates were reported by Bai et al. [12] and Ganor et al. [29], after heat treatment at 950 °C and 1050 °C, respectively.

When heat treatment was performed above the β-transus at 1000 °C for 2 h, the martensite α′ phase was fully transformed into a mixture of lamella α + β phases, with the columnar grains no longer visible as can be seen in Figure 2(e). From the phase diagram in Figure 3, 1000 °C is regarded as a temperature above β-transus for Ti6Al4V, which implies that the martensite α′ phase was fully transformed into β phase upon heating and transformed back to lamella α + β phases upon cooling [14,23]. This observation accounts for the disappearance of the columnar prior β grains in Figure 2(e). The transformation from β phase to α + β (β → α +β) occurred through diffusional process upon cooling from the β phase field [6)]. In addition, heat treatment at 1000 °C promoted the formation of β phase precipitates as seen in Figure 2(f) compared to the resulting microstructure that formed in sample that was heat

treated at 950 °C. It must be noted that a slight increase in grain size of the α + β phases was observed after heat treatment at 1000 °C as can be seen in both Figures 2(e) and 2(f). The slight increase in grains was attributed to the difference in temperatures between 950 °C and 1000 °C.

Refinement of the columnar β grains into equiaxed morphology was evident after heat treatment at 1000 °C for 8 h, as presented in Figure 2(g). It was obvious that the observed change was due to the longer residence time of 8 h. This heat treatment further led to the deformation of the β grain, which resulted in the formation of basketweave morphology with colonies of lamella α + β structure, found inside the large equiaxed grains as can be seen in Figure 2(g). According to Zou et al. [24], epitaxial recrystallisation is the suggested mechanism for the refinement of the columnar morphology to equiaxed, whereby high-density dislocation in the as-built state would initiate epitaxial recrystallisation of α grain inside the prior β grain. This observation was confirmed by Vrancken et al [27] and Chicos et al. [30] who reported that large colonies are possible over longer residence times. Furthermore, thinner lamella α grains were observed (Figure 2h) and this was due to the change in morphology from columnar to equiaxed grains of the parent β grain. A similar type of microstructure was reported by Sieniawki et al. [31]. From the study it was observed that the parent β grain, size of α-colonies and size and thickness of the α + β lamellae affect mechanical properties. Heat treatment at 1000 °C for 8 h resulted in the reduction of the β precipitates as depicted in Figure 2(g). However, a slight increase in size of the β precipitates as can be seen in Figure 2(h).

3.2 Hardness

The hardness profiles and average hardness of the as-built and heat-treated samples are shown in Figure 4 and Table 2, respectively.

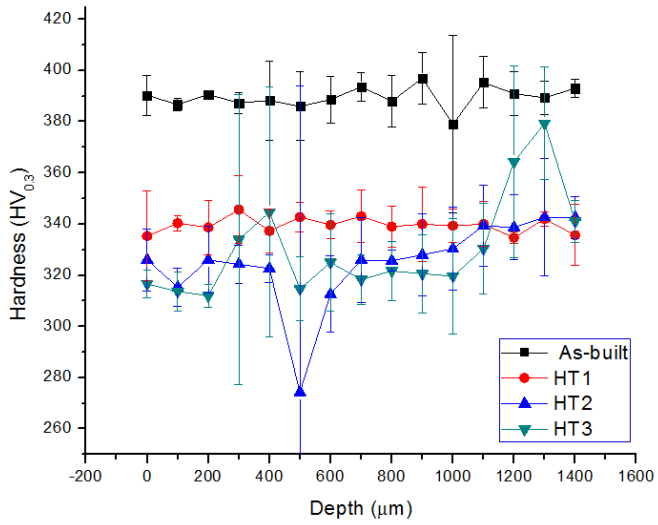

Fig. 4. Hardness profiles of the as-built and heat treated Ti6Al4V samples.

Table 2. Average hardness of the Ti6Al4V samples.

Sample	Hardness ($HV_{0.3}$)
As-built	389 ± 10
HT-1	340 ± 9
HT-2	325 ± 20
HT-3	330 ± 20

The as-built sample gave a linear and highest hardness profile as presented in Figure 5. The sample gave highest average hardness value of 389 ± 10 $HV_{0.3}$ as can be seen in Table 2. The high hardness of the as-built sample was attributed to the fully martensitic α′ structure that was observed on the microstructure in Figure 3(b) [23, 32]. Liu et al. [6] reported that the high hardness of the non-stable martensite α′ phase is attributed to the lattice strains due to deformed lattice structures incurred during its formation. In contrast, Yang et al. [33] attributed the high hardness of martensite α′ phase to high density dislocations. A significant decrease in hardness profiles and average hardness value of 340 ± 9 $HV_{0.3}$ was observed after heat treatment at 950 °C as presented in Figure 5 and Table 2. This decrease in hardness was associated with the phase transformation from a fully martensitic α′ microstructure (Figure 2b) to a lamella α + β microstructure (Figure 2c, d). It is noteworthy that sample that was heat treated at 950 °C gave a linear hardness profile.

Heat treatment at 1000 °C for 2 h resulted in a further decrease in hardness to 325 ± 20 $HV_{0.3}$. There are two factors that were understood to have led to this observation. The first one was the slight grain growth that was observed after heat treatment (Figure 2f). The relationship between hardness (HV) and the size of the grain (D) can be expressed according to the Hall-Petch equation (Equation 1) [34].

$$HV = HVo + kD^{-0.5} \quad (1)$$

Where HV_0 and k are material constant representing the hardness of a grain free material and hardening coefficient, respectively. This implies that an increase in grain size leads to a decrease in hardness. The second factor was the increase in the amount of β precipitates that were observed on the microstructure in Figure 3(e). As a result, heat treatment at 1000 °C for 2 h gave the lowest average hardness value of 325 ± 20 $HV_{0.3}$. There was not much hardness variation observed between hardness of the sample that was heat treated at 1000 °C for 2 h and 8 h. However, a slight increase to 330 ± 20 $HV_{0.3}$ was evident as presented in Table 2.

3.3 Tensile properties

Figure 5 and Table 3 show the engineering tensile stress-strain curves and a summary of mechanical properties of the samples, respectively. Three samples were tested and plotted for each heat treatment profile.

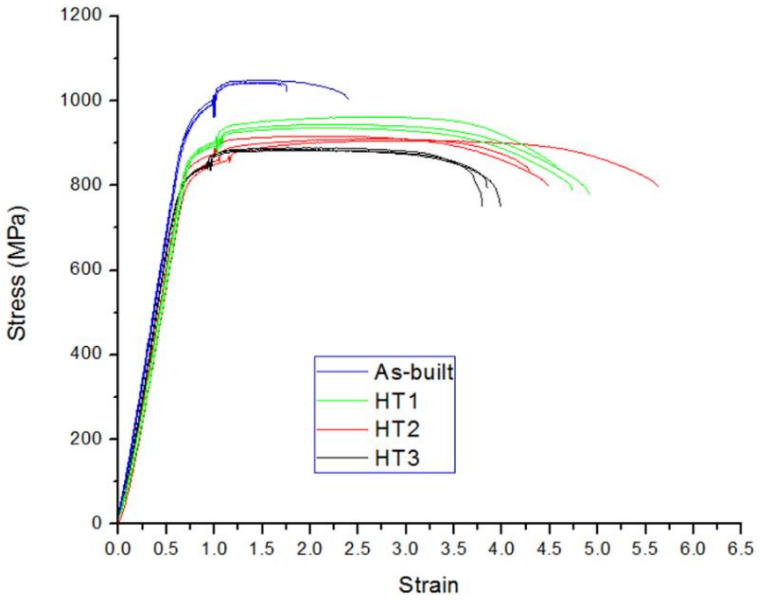

Fig. 5. Stress versus strain curves of the samples.

Table 3. Tensile properties of the samples.

Sample	YS (MPa)	UTS (MPa)	Ductility (%)
As-built	949 ± 10	1045 ± 3	5 ± 1
HT-1	872 ± 4	948 ± 13	13 ± 5
HT-2	835 ± 11	911 ± 5	13 ± 2
HT-3	807 ± 2	886 ± 3	13 ± 1
ASTM [37]	<795.00	<860.00	<10.00

It can be seen from Figure 5 and Table 3 that as-built sample gave the lowest ductility of 5%. However, the as-built sample gave the highest yield strength (YS) and ultimate tensile strength (UTS) of 948.81 ± 10 MPa and 1045.22 ± 3 MPa, respectively. Since the microstructure is known to directly governs the mechanical properties [8], the low ductility was attributed to the presence of the martensitic α′ phase on the microstructure of the sample (Figure 2b) [6, 20, 27]. Similar results of high YS and UTS and low ductility on SLM manufactured Ti6Al4V was reported in literature [20, 35, 36]. According to ASTM standard F2924-14 [37], the minimum required values for YS and UTS are 795 MPa and 860 MPa, respectively, while ductility is required to be at least 10% for Ti6Al4V parts produced with additive manufacturing technology (Table 3). This implies that even though the as-built sample gave highest YS and UTS, the ductility was below the required ASTM standard.

Heat treatment at 950 °C resulted in a major ductility increase to 13% as can be seen in Figure 5 and Table 3. However, the ductility increase was followed by a decrease in YS and UTS to 872 ± 4 MPa and 948 ± 13 MPa, respectively. The increase in ductility together with drop in YS and UTS was attributed to the phase transformation from fully martensitic α′ structure to lamella α + β structure (Figure 2d) [36]. A study by Munir et al. [38] reported an improved ductility on a lamella α + β microstructure.

Heat treatment at 1000 °C for 2 h resulted in a further decrease of YS and UTS to 835 ± 11 MPa and 911 MPa, respectively, with ductility remaining the same as 13% as presented in Table 3. This decrease in strength was attributed to the slight grain growth that was observed on the microstructure in Figure 2(f), caused by the difference in temperatures between 950 °C and 1000 °C [28]. A major change in strength was observed after heat treatment at 1000 °C for 8 h, whereby a further decrease in YS and UTS to 809 ± 2 MPa and 886 ± 3 MPa, while ductility remained at 13% as can be seen in Table 3. However, it must be noted that all the heat treatments conducted in this study gave YS, UTS and ductility that was within the required ASTM standard for additively manufactured Ti6Al4V. Similar trends highlighting the effect of heat treatment on tensile properties (i.e., yield strength, ultimate tensile strength, and ductility) on Ti6Al4V alloy are reported in literature [42,45]. A further study on the fractured surface of all the samples was conducted and the results are presented in the next section.

3.4 Fracture

Figure 6 present the SEM micrographs of tensile fracture morphology of as-built and heat treated samples.

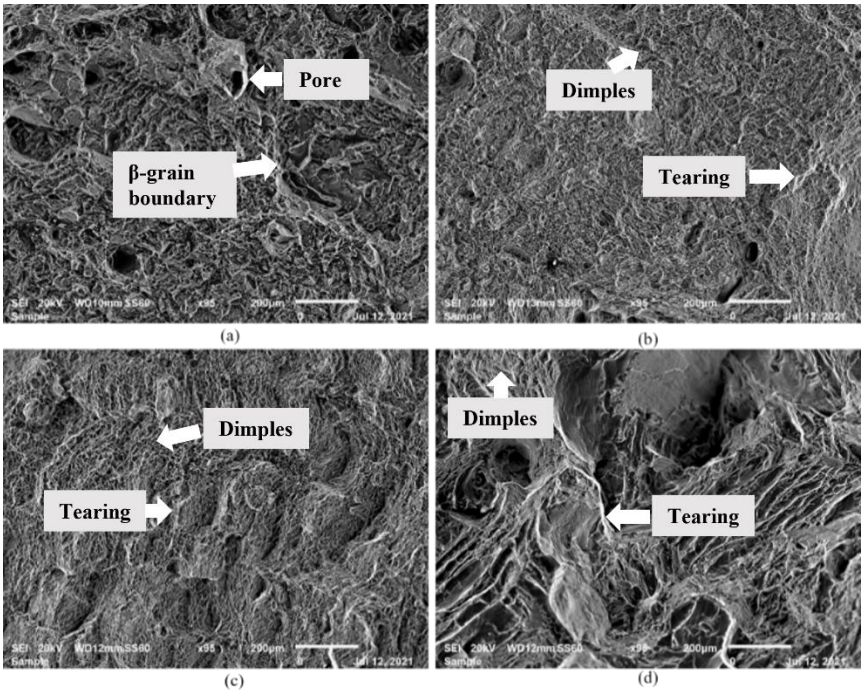

Fig. 6. SEM micrographs as-built and heat treated Ti6Al4V samples.

Figure 6(a) shows that the crack failure of the as-built sample propagated through the columnar prior β grain, which was an indication of a brittle fracture. This observation was in

agreement with the lowest ductility that was observed in Figure 5 and Table 3, due to the martensitic α′ structure. The brittle nature of the as-built sample was obviously associated with the fully martensitic α′ structure (Figure 3b). In addition, the as-built sample showed the presence of micro-pores as shown in Figure 6(a). It is understood that these microspores might influence the tensile properties by acting as multiple stress concentrators that can lead to elongation failure or crack initiation [39]. On the other hand, all the heat-treated samples showed the presence of tearing ridges in the fractured surfaces, indicating a ductile behaviour before final fracture occurred. Moreover, finer dimples were also observed on the fractured surface of the heat-treated samples as shown in Figures 6(b, c, d), which was a clear indication of a ductile fracture [40]. This observation aligned with the increased ductility that was observed on stress-strain curves in Figure 5 and Table 3.

4 Conclusion

This study undertook to understand the effect of post heat treatment on the microstructure, hardness, and tensile properties of Ti6Al4V samples fabricated with high speed SLM. Several heat treatments were performed at temperatures slightly below and above β transus temperature of Ti6Al4V. It was demonstrated that heat treatment at both 950 °C and 1000 °C influenced the microstructure and mechanical properties of SLM built Ti6Al4V parts. The results arrived at the following conclusions:

- Heat treatment at 1000 °C for 2 h produces a lamella α + β microstructure that offers a promising good balance of hardness, YS, UTS and ductility.
- Heat treatment at 950 °C and 1000 °C result in a major increase in ductility, followed by a noticeable decrease in hardness, YS and UTS.
- Heat treatment at 1000 °C for 8 h lead to formation of a basket weave microstructure, followed by a major reduction in YS and UTS.

Acknowledgements

The authors would like to thank CSIR and the University of Pretoria for laboratory and equipment support. the Department of Science and Innovation (DSI) of South Africa is acknowledged for financial support through the Collaborative Program in Additive Manufacturing (CPAM).

References

1. N. Jin, Z. Yan, Y. Wang, H. Chen, H. Zhang, Int. J. Mech. Sci. **190**, (2021)
2. M. Pham, C. Liu, L. Todd, J. Lertthanasarn, Nature. **565**, (2019)
3. A. Barnejee, D. Bernoulli, H. Zhang, M. Yuen, J. Liu, J. Dong, D. Feng, Science **360**, (2019)
4. A.A. Zadpoor, R. Hadeyati, Ann. Biomed. Eng. **45**, (2017)
5. R. Wauthle, S.M. Ahmadi, S.A. Yavari, Mater. Sci. Eng C. **54**, (2015)
6. S. Liu, Y.C. Shin, Mater. Des. **164**, (2019)
7. T. Childerhouse, M. Jackson, Metals. **9**, (2012)
8. Z. Wang, K. Guan, M. Gao, J. Alloys Compd. **513**, (2012)
9. C.Y. Yap, C.K. Chua, Z.L. Dong, Z.H. Liu, D.Q. Zhang, L.E. Loh, S.L. Sing, Appl. Phys. Rev. **2**, (2015)

10. P.M. Lekoadi, N. Maledi, M. Tlotleng, B.N. Masina, *Investigation of microstructural characteristics of heat treated high speed selective laser melted Ti6Al4V components*, in proceeding of the RAPDASA conference, 6-9 November 2018, Johannesburg, South Africa (2018)
11. N. Eshawish, S. Malinov, S. Wei, P. Walls, J. Mater. Eng. Perform. **10**, (2021)
12. H. Bai, H. Deng, L. Chen, X. Liu, X. Qin, D. Zhang, T. Liu, X. Cui, Metals. **11**, (2021)
13. R.J. Herbert, J. Mater. Sci. **51**, (2016)
14. P.M. Lekoadi, N. Maledi, M. Tlotleng, B.N. Masina, *Improving the microstructure of high speed selective laser melted Ti6Al4V components by varying residence time during heat treatment*, in proceeding of the RAPDASA conference, 6-8 November 2019, Bloemfontein, South Africa (2018)
15. X.P. Tan, Y. Kok, Y.J. Tan, Acta Mater. **97**, (2015)
16. W. Xu, M. Brandt, S. Sun, J. Elambasseril, Q. Liu, K. Latham, K, Xia, M. Qian, Acta Mater. **85**, (2015)
17. Z.N. Xiao, T.T. Liu, W.H. Liao, Chin. J. Lasers. **44**, (2017)
18. P.M. Lekoadi, N. Maledi, M. Tlotleng, B.N. Masina, *Investigation of martensite α' phase transformation during heat treatment of high-speed selective laser melted Ti6Al4V components*, in proceeding of The Mineral, Metals & Materials 149th annual conference, TMS, 23-27 February 2020, San Diego, USA (2020)
19. M. Yan, P. Yu, Sinter. Tech. Mater. **23**, (2015)
20. G.M. Ter Haar, T.H. Becker, Materials, **11**, (2018)
21. R. Sabban, S. Bahl, K. Chatterjee, S. Suwan, Acta Mater. **162**, (2019)
22. H. Li, Z. Zhao, Y. Ning, H. Guo, Z. Yao, Metals, **8**, (2018)
23. P. Lekoadi, M. Tlotleng, K. Anna, N. Maledi, B. Masina, Metals, **11**, (2021)
24. Z. Zou, M. Simonelli, J. Katrib, G. Dimitrakis, R. Hague, Mater. Sci. Eng. A. **814**, (2021)
25. H. Li, Z. Zhao, Y. Ning, H. Guo, Z. Yao, Metals, **8**, (2018)
26. S.Q. Wu, Y.J. Lu, Y.L. Gan, T.T. Huang, C.Q. Zhao, J.J. Lin, S. Guo, J.X. Lin, J. Alloys Compd. **672**, (2016)
27. B. Vracken, L. Thijs, P.J. Kruth, J. Van Humbeeck, J. Alloys Compd. **451**, (2012)
28. M. Jia, Y. Alshammari, F. Yang, L. Balzoni, Mater. Sci. Eng. A. **791**, (2020)
29. Y.I. Ganor, E. Tiferet, S.C. Vogel, D.W. Brown, M. Chonin, A. Pesach, Materials, **14**, (2021)
30. L.A. Chicos, S.M. Zaharia, C. Lancea, M.A. Pop, I. Canadas, J. Rondriguez, J. Galindo, J. Sol. Energy, **173**, (2018)
31. J. Sieniawski, W. Ziaja, K. Kubiak, M. Motyka, Titanium alloys (InTech, 2013)
32. A. Gupta, R.K. Khatirkar, A. Kumar, M.S. Parihar, J. Mater. Res. Soc. **54**, (2018)
33. J. Yang, H. Yu, J. Yin, M. Gao, Z. Wang, X. Zeng, Mater. Des. **108**, (2016)
34. J.S. Zuback, T. Debroy, Materials, **11**, (2018)
35. X. Zhang, G. Fang, S. Leeflang, A.J. Bottger, A.A. Zadpoor, J. Zhou, J. Alloys. Compd. **735**, (2018)
36. J. Tong, C.R. Bowen, J. Persson, A. Plummer, Mater. Sci. Tech. **33**, (2017)

37. ASTM F2924-14, (2012), *Standard Specification for Additive Manufacturing Titanium-6 Aluminum-4 Vanadium with Powder Bed Fusion*, ASTM International, West Conshohocken, PA.
38. K.S. Munir, Y. Zheng, D. Zhang, J. Lin, Y. Li, C, Wen, Mater. Sci. Eng. A. **688**, (2017)
39. E. Tiferet, M. Ganor, D. Zolotaryov, A, Garkun, A. Hadjadj, M. Chonin, O. Yeheskel, Materials, 12, (2019)
40. X. Gong, K. Anderson, K. Chou, Manuf. Rev. **1**, (2012)